REGULAR ARTICLE

Polymer Journal

Special Issues –International Symposium on Polymer Crystallization 2007–

Directional Entropy of Chain Folding Detected in Chain Folding Free Energies? Crystal Thickness Transition of *isotactic* Polybutene-1 Tetragonal Phase

By Motoi YAMASHITA and Takuya TAKAHASHI*

Lamellar crystal thickness l_c of *isotactic* polybutene-1 (*it*-PB1) has been investigated for crystallization in the melt over a wide range of crystallization temperature T from 40 to 90 °C by small angle X-ray scattering experiments and density measurements. The crystal thickness l_c demonstrates two linear dependences on inverse supercooling and a transition from one dependence to the other has been observed around $T = 65$ °C. Each of the two dependences obeys the nucleation theory in the high and low supercooling ranges, respectively. Chain folding free energy q determined from the low supercooling range is larger than that determined from the high supercooling range. We discuss possible mechanisms for the transition taking account of entropy of chain folding directions and propose that the difference in the q values could be due to the change in directional entropy of chain folding caused by kinetic roughening.

KEY WORDS: *Isotactic* Polybutene-1 / Tetragonal Phase / Melt Crystallization / Crystal Thickness / Chain Folding Direction / Small Angle X-ray Scattering /

In the crystallization of polymers, polymer chains in the form of random coils develop into double layer structures composed of folded chain crystals (lamellar crystals) and amorphous layers. Lamellar crystal thickness is the most important quantity describing the morphology specific to polymer crystals. The nucleation theory by Hoffman *et al.*[1,2] explains that crystal thickness of polymers is determined kinetically, and gives the observed dependence of lamellar thickness l_c on supercooling $\Delta T = T_m{}^0 - T$ ($T_m{}^0$ is the equilibrium melting temperature, T is the crystallization temperature) by the following equation; l_c shows a single linear dependence on inverse supercooling, $1/\Delta T$.

$$l_c = \frac{A}{\Delta T} + \delta l \equiv l_c^* + \delta l_c \tag{1}$$

where A and δl_c are constants. According to the theory, A is expressed as follows:

$$A = \frac{2\sigma_e T_m^0}{\Delta h_f} \tag{2}$$

Here, σ_e is the end-surface free energy per unit area of polymer crystals and Δh_f the heat of fusion per unit volume of the crystal phase. The first term $l_c{}^* = 2\sigma_e T_m{}^0/\Delta h_f \Delta T$ in eq 1 represents the minimum lamellar crystal thickness to keep the crystal thermodynamically stable, and the second term corresponds to the driving force of crystallization. Hence, crystal thicknesses of semicrystalline polymers reflect the processes of their structure formation.

Recently, Fu *et al.*[3] observed a deviation from the nucleation theory in the temperature dependence of crystal thickness of *isotactic* polybutene-1 (*it*-PB1) determined from electron density correlation analysis of small angle X-ray scattering (SAXS) profiles. They observed that two different relationships exist between crystal thickness l_c and crystallization temperature T, and that transition from one relationship to the other occurs, *i.e.*, l_c increases discontinuously accompanied by a morphological change of crystals when l_c becomes roughly equal to the chain dimensions. They also showed that crystals with two different kinds of thicknesses co-exist around the transition temperatures and the temperature dependence of crystallization half-time shows some kind of transition.

We have reinvestigated this transition in terms of more simple methods, using *it*-PB1 with different molecular weight distribution from that used in the study by Fu *et al.* as samples.[4] We have studied the temperature dependence of lamellar crystal thicknesses of *it*-PB1 tetragonal crystals grown in the melt by SAXS experiments and crystallinity measurements. *It*-PB1 is a semicrystalline polyolefin with ethyl side-groups. *It*-PB1 exhibits stable trigonal form with 3/1 helical chains and metastable tetragonal form with 11/3 helical chains as the most common structures, as shown in Table I.[5–9] Crystallization in the bulk melt under atmospheric pressure yields the tetragonal form.[10] Due to the metastability of the tetragonal form, the solid-solid spontaneous transformation to the stable trigonal form then takes place in several days after cooling to room temperature.[5]

In this study, we found another kind of crystal thickness transition. We again observed two different temperature dependences of crystal thickness l_c, but the transition between the two dependences was observed in a temperature range where l_c is half the chain dimensions Fu *et al.* defined. This is quite different from the transition reported by Fu *et al.* We also

Department of Bioscience and Bioinformatics, Ritsumeikan University, 1-1-1 Noji-higashi, Kusatsu 525-8577, Japan
*To whom correspondence should be addressed (Present address: Department of Pharmacy, Ritsumeikan University, Tel: +81-77-561-2658, Ext. 8427, Fax: +81-(0)77-561-2659, E-mail: motoi-y@fc.ritsumei.ac.jp).

 doi:10.1295/polymj.PJ2007198

Table I. Physical Properties of *it*-PB1

	Unit Cell Parameters			ρ^c	Stem Parameters		l_u	l_b
	a_0 (Å)	b_0 (Å)	c_0 (Å)	(g cm^{-3})	a (Å)	b (Å)	(Å)	(Å)
Trigonal[a]	17.7	17.7	6.5	0.96	5.1	8.85	1.08	
Tetragonal[b]	14.6	14.6	21.2	0.888	7.3	7.3	0.964	
Amorphous				0.87				1.54

Continued

	Δh_f^d (J m^{-3})	$T_m^{0\,d,e}$ (°C)	Space group	Chain Conformation (monomers/turn)
Trigonal	1.35×10^8	124.0	$R\bar{3}c$	3/1
Tetragonal	1.09×10^8	136.1	$P\bar{4}b2$	11/3

[a]From ref. 5. [b]From ref. 6. [c]From ref. 7. [d]From ref. 8. [e]From ref. 9.

observed two linearities in the inverse supercooling dependence of l_c, which indicate that each of the two relationships still obeys the nucleation theory. We are going to discuss possible mechanisms for the transition taking account of entropy of chain folding directions.

EXPERIMENTAL

The *it*-PB1 used in this study was purchased from Scientific Polymer Product. Weight-averaged molecular weight M_w and number-averaged molecular weight M_n determined with gel permeation chromatography (GPC) calibrated by polystyrene standard samples are $M_w = 277300$ and $M_n = 60340$, respectively.

We measured the density ρ of samples by float and sink method using mixed solvents of water and ethanol at 25 °C; crystallinity ϕ was determined from the density using the following equation.

$$\rho = \rho_c\phi + \rho_a(1 - \phi) \tag{3}$$

where ρ_c and ρ_a are the density of crystalline and amorphous phases, respectively, listed in Table I.

SAXS photographs were taken with a SAXS camera (camera length 414 mm) in vacuum to obtain lamellar long periods, using an imaging plate system (Rigaku R-AXIS DS-II). X-Ray used was nickel-filtered CuK_α radiation generated at 50 kV and 140 mA. After the subtraction of the background intensity, isotropic two-dimensional data were circularly averaged to obtain one-dimensional data, and corrected for the Lorentz factor. The first- and second-order reflections were separated by fitting SAXS profiles with Gaussian-Lorentzian product functions by GRAMS Research Version 3.01B (Galactic Industries Corporation). Application of Bragg's law to the scattering peak centers was used to calculate the first- and second-order long periods, L_1 and L_2. The lamellar crystal thickness l_c was estimated using the equation: $l_c = \phi L_1$.

Films of *it*-PB1, about 500 µm in thickness, between aluminum foil were melted at 150 °C for 3 min in an oven, transferred quickly to a hot-stage (Mettler FP82) kept at a crystallization temperature between 40 °C and 90 °C. The films crystallized were aged at room temperature for 10 d and used for SAXS and density measurements. In 10 d of aging at room temperature the tetragonal crystals transform into the trigonal form without changing their stacked lamellae structure and overall mass degree of crystallinity. Since the crystal density of the trigonal form is larger than that of the tetragonal form, SAXS intensity is much enhanced after 10 d. We determined l_c of the aged samples, then calculated l_c of the as-crystallized tetragonal samples from the observed values of l_c of the aged samples assuming that l_c(as-crystallized) = l_c(aged)/1.12. This assumption is based on the fact that the tetragonal-trigonal transformation involves an extension of the 11/3 helical conformation (tetragonal form) into the 3/1 helix (trigonal form). The ratio between the axial repeating units of the two conformations is of 1.12.

Wide angle X-ray scattering (WAXS) was performed to identify crystal structures for samples within 5 min after crystallization followed by quenching and samples stored at room temperature for 10 d after crystallization. X-Ray used was nickel-filtered CuK_α radiation generated at 35 kV and 40 mA. The system and procedure used for data acquisition and analyses were the same as those used for SAXS experiments.

RESULTS

We confirmed by WAXS measurements that samples within 5 min after the crystallization followed by quenching were in the tetragonal form (the three profiles designated by "As crystallized" in Figure 1). Hence the observed crystallinities and lamellar crystal thicknesses reflect those of tetragonal crystals. Samples aged at room temperature for 10 d exhibited peaks characteristic of the trigonal form.

Figure 2 shows the Lorentz-corrected SAXS profiles of the samples. First- and second-order reflections were observed in the wide range of crystallization temperature from 40 °C to 90 °C. Table II lists the results of SAXS and crystallinity

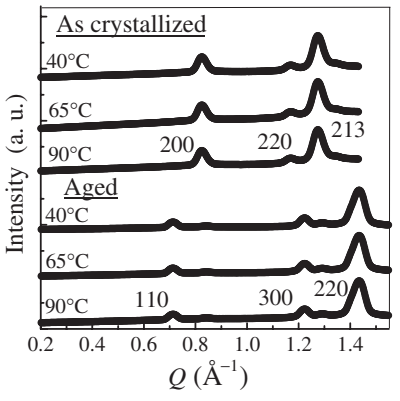

Figure 1. WAXS profiles of *it*-PB1 crystallized at 40 °C, 65 °C, and 90 °C plotted against the modulus of the scattering vector Q. ($Q = 4\pi\lambda^{-1}\sin\theta$, θ is half the scattering angle, λ is the wave length used.) The profiles for samples as crystallized (within 5 min after the crystallization followed by quenching) and aged are plotted. Peaks shown in the plots of as crystallized samples are indexed with 200, 220, 213 reflections of the tetragonal form; peaks exhibited in the plots of the aged samples are indexed with 110, 300, 220 reflections of the trigonal form.

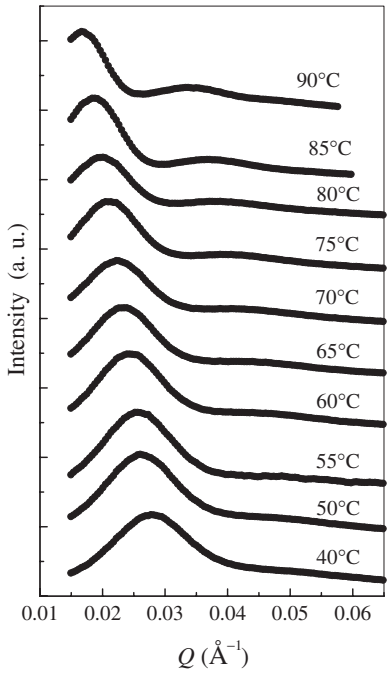

Figure 2. SAXS profiles of *it*-PB1 samples crystallized at temperatures from 40 °C to 90 °C. The profiles have been shifted vertically for clarity.

Table II. Results of SAXS and Crystallinity Measurements

T_c (°C)	L_1 (Å)	L_2 (Å)	ϕ (%)	l_c (Å)
40	222	125	46.7	92.7
50	237	130	46.1	97.6
55	247	133	46.6	102
60	258	136	46.7	106
65	267	141	49.2	117
70	281	146	51.7	130
75	297	158	51.7	137
80	319	170	54.2	154
85	334	171	54.2	162
90	368	182	55.9	184

T_c = crystallization temperature, L_1 = the first-order long periods, L_2 = the second-order long periods, ϕ = crystallinity, l_c = lamellar crystal thickness. The l_c data are estimated values of as-crystallized samples before aging; they were derived assuming l_c(as-crystallized) = l_c(aged)/1.12. (See the text.).

measurements: crystallization temperatures, the values of the first- and second-order long periods, degree of crystallinity, and lamellar crystal thickness.

Figure 3 shows the lamellar crystal thickness l_c plotted as a function of the inverse supercooling, $1/\Delta T$. ($\Delta T = T_m^0 - T$; the equilibrium melting temperature T_m^0 is 124 °C for *it*-PB1 tetragonal phase, as shown in Table I.) The dependence clearly deviates from a single linearity. Two linear relationships between l_c and $1/\Delta T$ can be observed, one in the low ΔT range ($1/\Delta T = 0.018$–$0.030\,K^{-1}$; this corresponds to $T = 90$–70 °C) and the other in the high ΔT range ($1/\Delta T = 0.012$–$0.016\,K^{-1}$; this corresponds to $T = 60$–40 °C). When $1/\Delta T$ increases from the high ΔT range to the low ΔT range, l_c moves up from the lower line to the upper line in Figure 3. This

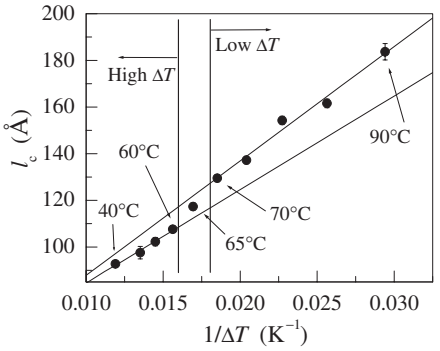

Figure 3. Lamellar crystal thickness l_c as a function of the inverse supercooling, $1/\Delta T$.

seems similar to the observation reported by Fu *et al.* At $1/\Delta T = 0.017\,K^{-1}$, l_c locates in the middle of the two linearities, which suggests a transition state between the two linear relationships. According to the eqs 1 and 2, the extrapolation to $1/\Delta T = 0\,K^{-1}$ of the straight lines in Figure 3 gives the values of δl_c to be 38.8 ± 8.4 Å for the low ΔT range and 44.3 ± 4.8 Å for the high ΔT range. The slopes give the values of $2\sigma_e T_m^0/\Delta h_f$ to be $(4.90 \pm 0.39) \times 10^3$ Å K for the low ΔT range and $(4.01 \pm 0.35) \times 10^3$ Å K for the high ΔT range; σ_e is estimated as $(6.73 \pm 0.49) \times 10^{-2}\,J\,m^{-2}$ for the low ΔT range and $(5.51 \pm 0.48) \times 10^{-2}\,J\,m^{-2}$ for the high ΔT range, using the values of Δh_f and T_m^0 given in Table I. Chain folding free energies $q = 2ab\sigma_e$ (a and b represent the height and width of a stem, respectively; the values are shown in Table I.) are calculated as $(7.17 \pm 0.52) \times 10^{-20}$ J stem^{-1} for the low ΔT range and $(5.87 \pm 0.51) \times 10^{-20}$ J stem^{-1} for the high ΔT range.

DISCUSSION

We observed two different dependences of l_c on $1/\Delta T$ and the transition between them; l_c depends linearly on $1/\Delta T$ in each of the low and high supercooling ranges. The two linearities we observed in the $1/\Delta T$ dependence of l_c indicate that the dependences obey the nucleation theory in each of the high and low ΔT ranges. The slope of l_c *vs.* $1/\Delta T$ plot is proportional to the end surface free energy σ_e of crystals, *i.e.*, it reflects the free energy $q = 2ab\sigma_e$ of chain folding. The q value determined from the low ΔT range is larger than that determined from the high ΔT range by 1.30×10^{-20} J stem^{-1}, which amounts to 22% of the q value in the high ΔT range. We need to explain the difference between the q values in the high and low supercooling ranges.

Crystal thickness transition and the difference between the two q values determined from the slopes in l_c *vs.* $1/\Delta T$ plot can be explained by the change of chain folding directions caused by kinetic roughening. Below we consider the number of possible combinations of chain folding directions at one end and the opposite end of a stem. We distinguish the chain folding direction at one end of a stem from that at the opposite end of the stem by designating them as "folding-in" direction

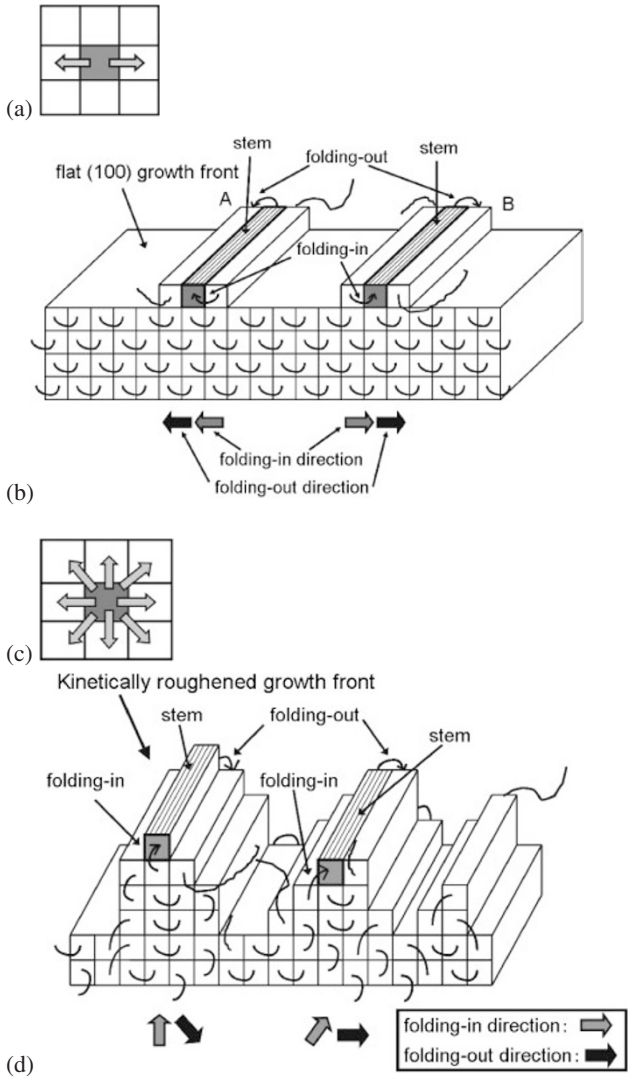

Figure 4. (a) Schematic illustration of chain re-entrant sites in facetted crystals seen from the crystalline *c*-axis. (b) Chain folding directions on facetted crystal growth front. Since chain re-entrant sites are restricted to the 2 neighboring stems along the (100) growth front, there are only two combinations of chain folding-in and chain folding-out directions shown as A and B. (c) Schematic illustration of chain re-entrant sites in kinetically roughened crystals seen from the crystalline *c*-axis. (d) Chain folding on kinetically roughened growth front. Since the growth front is rough, chain re-entrant sites can be neighboring 8 stems. Chain can fold-in from neighboring 8 stems and can fold-out into neighboring 7 stems. The number of possible combinations of chain folding-in and folding-out directions is 8 × 7 = 56.

and "folding-out" direction, as shown in Figure 4. (We first assume that chain folding possesses only adjacent or next-nearest adjacent re-entry.) *It*-PB1 tetragonal crystals have facetted morphology indicative of flat growth fronts in the molecular scale at lower ΔT, while they present rounded morphology with kinetically roughened growth front in the molecular scale[10,11] at higher ΔT. In facetted crystals of the tetragonal phase, chain folding directions are restricted to those parallel to the (100) growth front (Figure 4a, 4b) within each (100) sector since step propagation occurs along the (100) growth front during the crystallization process. A chain can fold from one stem in the lattice to its two adjacent stems along the (100) plane. Hence, the number of combinations of folding-in and folding-out directions is 2, as shown in Figure 4b. On the contrary, in kinetically roughened crystals, chain folding directions are no longer restricted to (100) directions (Figure 4c, 4d); a chain can fold-in from 8 neighbouring stems, and can fold-out into the rest 7 neighbouring stems (Figure 4d). (Notice that the chain can not return to the same stem that it came from.) Hence, the number of combinations of folding-in and folding-out directions is estimated to be $8 \times 7 = 56$, assuming that the re-entries into the 8 stems have the same probabilities. With increasing temperature, the growth front changes from rounded to facetted morphology, which reduces the number of combinations of folding-in and folding-out directions from 56 to 2. Reduced number of combinations of folding-in and folding-out directions causes the reduction of configurational entropy of re-entrant sites of folded chains, and this shows up as the difference between the chain folding free energy values. The configurational entropies of combination of chain folding-in and folding-out sites for facetted and kinetically roughened growth fronts are estimated to be $k \ln 2$ stem^{-1} and $k \ln 56$ stem^{-1}, respectively. The reduced entropy of chain folding-in and folding-out sites of facetted growth fronts as measured relative to roughened growth fronts is calculated to be $k \ln 28$. This corresponds to the free energy difference of 15.5×10^{-21} J stem^{-1} at 65 °C. This value is roughly in agreement with the difference of the q values, 13.0×10^{-21} J stem^{-1}. The agreement indicates that the observed change of the slope in the $1/\Delta T$ dependence of l_c is caused by the change of entropy of chain folding directions.

We next consider the effect of non-adjacent re-entries. Non-adjacent re-entries do not bring about a large change in the difference of chain folding energies, as shown below. The chain folding of non-adjacent re-entries is looser than that of adjacent re-entries. Looser chain folding reduces the energy of chain folding for both of faceted and kinetically roughened crystals. If we assume the fraction of non-adjacent re-entries is the same for faceted and kinetically roughened crystals, the chain folding energy which results from the average of adjacent, next-nearest adjacent and non-adjacent folding would be roughly the same for faceted and kinetically roughened crystals. Hence in the difference between the q values, the reduction is cancelled. The decrease of chain folding energy due to loose folding is not considered to bring about a large change in the difference of q values.

Non-adjacent re-entries do not cause a large change in the difference of configurational entropy of chain re-entrant sites between faceted and kinetically roughened crystals. The sum of probabilities p_{tf} of adjacent and next-nearest adjacent re-entries has the lower limit of $1 - (\rho_a/\rho_c)(l_b/l_u)(1/3\cos\theta)$.[2] Here l_b is the C-C bond length, l_u the C-C distance as projected along the *c*-axis as listed in Table I, and θ is the angle of tilt of the *c*-axis as measured from the direction perpendicular to the lamellar end surface, which is 0° for *it*-PB1 tetragonal phase. The p_{tf} value is calculated to have the lower limit of 0.478. To make the calculations below simple, we set the p_{tf} value to be 0.5,

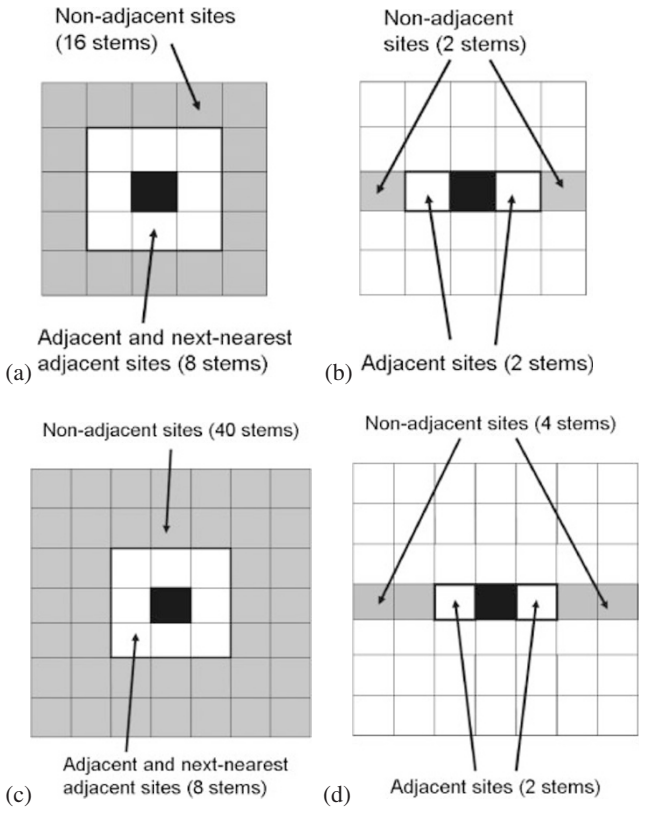

Figure 5. Schematic illustrations of chain re-entrant sites (a) in kinetically roughened crystals and (b) in facetted crystals seen from the crystalline *c*-axis when a chain re-entry can skip a stem. Non-adjacent sites are indicated by grey regions. Schematic illustrations of chain re-entrant sites (c) in kinetically roughened crystals and (d) in facetted crystals seen from the crystalline *c*-axis when a chain re-entry can skip 2 stems.

i.e., the sum of probabilities of adjacent and next-nearest adjacent re-entries is equal to that of non-adjacent re-entries. Here we consider a chain re-entry can skip a stem. In kinetically roughened crystals, potential chain re-entrant sites are 24 stems in a 5×5 grid (Figure 5a, 5b). In the 5×5 grid, non-adjacent sites are 16 stems at the periphery (the grey region of Figure 5a); adjacent and next-nearest adjacent sites are 8 stems around the center. We assume that each of the re-entries into the 16 stems at the periphery has an identical probability and that each of those into the 8 stems around the center has another identical probability. Since the sum of the probabilities of re-entries into the 8 stems around the center is equal to that of re-entries into the 16 stems at the periphery, the probability of the re-entry into each individual stem at the periphery is half that of the re-entry into each individual stem around the center. The relative population, r, of each individual non-adjacent re-entry as measured relative to the population of each individual adjacent or next-nearest adjacent re-entry is 0.5. The configurational entropy of chain re-entrant sites can be calculated by summing up the number of combinations of folding-in and folding-out sites weighted by the relative population r. In the case where none of the folding-in and folding-out sites belong to the 16 stems at the periphery, the number of combinations weighted by the relative population r is $8 \times 7 \times r^0 = 56$. In the case where either of the folding-in or folding-out sites belongs to the peripheral 16 stems, the number of combinations weighted by the relative population is $2 \times 8 \times 16 \times r^1 = 128$. In the case where both of the folding-in and folding-out sites belong to the peripheral 16 stems, the number of combinations weighted by the relative population is $16 \times 15 \times r^2 = 60$. Summing these up, the configurational entropy is calculated to be $k \ln(56 + 128 + 60) = k \ln 244$. In faceted crystals, potential chain re-entrant sites are 4 stems along the (100) plane; both of the adjacent and non-adjacent sites have 2 stems. Since the sum of the probabilities of re-entries into the adjacent 2 stems is equal to that of re-entries into the non-adjacent 2 stems, the probability of the re-entry into each individual non-adjacent stem is equal to that of the re-entry into each individual adjacent stem. The relative population r is unity. The number of combinations weighted by r is $2 \times 1 \times r^0 + 2 \times 2 \times 2 \times r^1 + 2 \times 1 \times r^2 = 12$; configurational entropy is $k \ln 12$. The difference in the configurational entropy is $k \ln 244 - k \ln 12 = k \ln 20.33$; this corresponds to the free energy difference of 14.06×10^{-21} J stem^{-1}. In the same way, when a chain re-entry can skip two stems, the potential chain re-entrant sites are 6 sites along the (100) plane and 48 sites in a 7×7 grid in faceted and kinetically roughened crystals, respectively (Figure 5c, 5d). In kinetically roughened crystals, non-adjacent sites are 40 stems at the periphery; the adjacent and next-nearest adjacent sites are 8 stems around the center. Since the sum of the probabilities of re-entries into the 8 stems around the center is equal to that of non-adjacent re-entries into the 40 stems at the periphery, the relative population r of non-adjacent re-entry is calculated to be $8/40 = 0.2$. The number of combinations weighted by the relative population is $8 \times 7 \times r^0 + 2 \times 8 \times 40 \times r^1 + 40 \times 39 \times r^2 = 246.4$; the configurational entropy is $k \ln 246.4$. In faceted crystals, adjacent sites and non-adjacent sites are 2 and 4 stems, respectively, as shown in Figure 5d. The relative population of a non-adjacent re-entry is calculated to be $r = 2/4 = 0.5$. The number of combinations weighted by the relative population r is $2 \times 1 \times r^0 + 2 \times 2 \times 4 \times r^1 + 4 \times 3 \times r^2 = 13$; configurational entropy is $k \ln 13$. The difference in the configurational entropy is $k \ln 246.4 - k \ln 13 = k \ln 18.95$; this corresponds to the free energy difference of 13.7×10^{-21} J stem^{-1}, which is even more excellent agreement with the difference of the q values.

In 2004, we determined the kinetic roughening temperature to be around 85 °C.[11,12] This is higher than the observed temperature of thickness transition, 65 °C. However, we also observed (100) sector boundaries in kinetically roughened crystals at 85 °C. The existence of sector boundaries indicates that the crystals have considerable fraction of (100) folding even in kinetically roughened state. This is considered to be due to the fact that surface nucleation process is still alive and step propagation along the (100) direction is working on kinetically roughened growth front, since the growth front is not thermally roughened. If we assume that the fraction of (100) folding undergoes a large decrease in the temperature range of 60–70 °C, we can account for the transition temper-

ature in the $1/\Delta T$ dependence of l_c. To confirm our hypothesis, we need to observe the (100) sector boundaries to disappear in this temperature range.

In our recent works,[9,13] we determined lateral surface free energy σ of *it*-PB1 trigonal and tetragonal crystals grown from the melt.[14–17] We showed that reduction of conformational entropy of ethyl side chains generates excessively larger value of σ of trigonal crystals than that estimated from Hoffman's theory of lateral surface free energy,[2] while the σ value of tetragonal crystals is in agreement with the theoretical estimation. The observed gap between the q values in the high and low supercooling ranges can be a new type of entropic effect of polymer crystal surfaces. We can postulate that the change in directional entropy of chain folding was detected in the difference between the q values.

The thickness transition observed in this work is considered to be different from that reported by Fu *et al.* We also performed *in situ* optical microscope observations of *it*-PB1 spherulites of the tetragonal phase in our previous work.[11] We could not observe such morphological change from spherulites to hedrites as reported by Fu *et al.* in the temperature range of 40–90 °C. Besides, the l_c value around the thickness transition temperature observed in this work is much smaller than the chain dimensions estimated from M_w, as we will show below.

Polymer chains are elongated along the crystal-melt interface before they become incorporated into the crystal phase. If the crystal thickness is smaller than the chain dimensions in the melt, Fu *et al.* simply hypothesized that crystallization does not necessary need a chain disentangling. Since chains become elongated and folded within the chain dimensions, the envelope of the volume occupied by the chains need neither to be elongated nor deformed. They therefore speculated that the entanglements can easily be shifted into the amorphous regions, where they can be accumulated together with the other noncrystallizable chain parts such as end groups and stereodefects. They called this process "folded-chain crystallization." (The "folded-chain crystallization" is easily envisioned to yield crystals described by "switchboard" model. For polyethylene crystallization, the "switchboard" type crystallization is reported to be almost impossible[2] because the p_{tf} value is reported to be as high as 0.81 from the computation on the basis of neutron scattering results.[18] As calculated above, the lower limit of the p_{tf} value of *it*-PB1 tetragonal phase is as low as 0.478; we can not deny the possibility of "folded-chain crystallization" so far.) An estimation of the chain dimensions in the melt is the radius of gyration R_g determined from M_w. Then, the condition for the crystallization without chain disentangling can be obtained as follows

$$l_c \leq R_g \tag{4}$$

If this condition is not satisfied, *i.e.*, if the crystal thickness is larger than R_g, they proposed that the chain needs to be disentangled to crystallize. They called this process "chain-extended crystallization."

For Gaussian chains, R_g and the mean-squared end-to-end distance R_0 are related by the following equation

$$R_g^2 = \frac{R_0^2}{6} \tag{5}$$

R_0 can be calculated using the characteristic ratio C_∞ as

$$R_0^2 = C_\infty a_b^2 N \tag{6}$$

Here, ${a_b}^2$ represents the sum of squares of the lengths of the backbone bonds in one monomer unit, and N is the degree of polymerization.

For *it*-PB1, C_∞ is given to be 18.0 in the literature;[19] ${a_b}^2$ is 4.74 Å^2. The degree of polymerization is calculated to be $4954 \equiv N_w$ from $M_w = 277300$. The radius of gyration is then estimated to be 266 Å $\equiv R_g$ from N_w. Fu *et al.* reported that l_c increases discontinuously accompanied by a morphological change from spherulites to hedrites when l_c becomes comparable to R_g. In the observed transition temperature range of 60–70 °C, the l_c value is 106–130 Å in this work, which is only half the value of $R_g = 266$ Å. Hence, the observed crystal thickness transition is different from that reported by Fu *et al.*

The difference between the transition reported by Fu *et al.* and that observed in this work is considered to originate from the difference in the crystallization temperature. The temperature range in which we performed crystallization, 40–90 °C, is lower than that in the work by Fu *et al.*, 85–108 °C; the molecular weight of the samples we used in this work ($M_w = 277{,}300$) is much larger than those of the samples ($M_w = 141{,}000$ and $185{,}000$) which presented the transition in the work by Fu *et al.* As the result, the range of the observed l_c values (92.7–184 Å) was too small to surpass the measure of chain dimensions, $R_g = 266$ Å. This is considered to be the reason why we could not observe the same transition that Fu *et al.* reported.

According to eq 1 with the values of the slope $A = 2\sigma_e {T_m}^0/\Delta h_f$ and δl determined for the low ΔT range, the l_c value is estimated to surpass the R_g value around 102.5 °C. We still need to perform crystallization up to the temperature higher than 102.5 °C and confirm if we could observe the same transition in crystal thickness and crystal morphology reported by Fu *et al.* We also need to investigate the temperature dependence of crystallization half-time, which was not performed in this study. A new study is already in preparation to observe the thickness of crystals formed at temperature higher than 102.5 °C by SAXS and atomic force microscopy.

For comparison, the l_c values reported in the work by Fu *et al.* are replotted as the function of $1/\Delta T$ in Figure 6. The dependence presents two kinds of linearities similar to those observed in this work. However, the two linear dependences are almost parallel. The slopes $A = 2\sigma_e {T_m}^0/\Delta h_f$ are calculated to be $(3.33 \pm 0.14) \times 10^3$ Å K for the lower ΔT range (95–108 °C) and $(3.63 \pm 0.15) \times 10^3$ Å K for the higher ΔT range (85–100 °C). Though the slope is somewhat smaller for the lower ΔT range, the difference in the slopes is almost within experimental errors. The model by Fu *et al.* does not generate the change of the q values, because disentanglement itself changes neither the energy of chain folding nor conformational

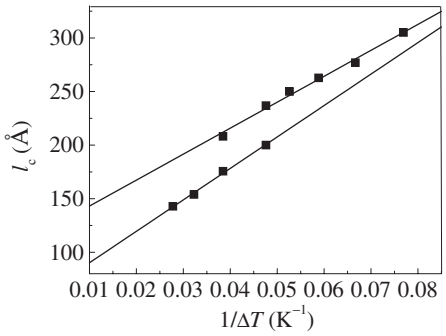

Figure 6. Lamellar crystal thickness l_c determined by Fu *et al.* is replotted as a function of the inverse supercooling, $1/\Delta T$. ($T_m^0 = 124\,°C$ is used to calculate the ΔT values.) Though the temperature dependence of the l_c values was not analyzed according to the nucleation theory in the work by Fu *et al.*, this plot indicates that the l_c value determined by Fu *et al.* obeys the nucleation theory in each of the lower ΔT range and higher ΔT range.

entropy of polymer chains. The same value of q yields the same values of the slopes in the l_c *vs.* $1/\Delta T$ plot. The almost parallel two lines in Figure 6 are consistent with the model by Fu *et al.* and support the fact that the transition observed in this work is different from that reported in their work.

CONCLUSION

We have investigated lamellar crystal thickness l_c of *it*-PB1 for crystallization in the melt over a wide range of crystallization temperature T from 40 to 90 °C by small angle X-ray scattering experiments and density measurements. The crystal thickness l_c demonstrated two linear dependences with different slopes on inverse supercooling and a transition from one dependence to the other was observed around $T = 65\,°C$. Each of the two dependences obeyed the nucleation theory in the high and low ΔT ranges, respectively.

Chain folding free energy q determined from the low ΔT range is larger than that determined from the high ΔT range by 1.30×10^{-20} J stem^{-1}. The transition observed in this work is considered to be different from that reported by Fu *et al.*, since the model proposed by them can neither account for the transition temperature nor the difference between the q values. The l_c value around 65 °C is only half the R_g value of *it*-PB1 samples used in this work. The difference can be explained by the change in chain folding directions caused by kinetic roughening. At lower ΔT, chain folding directions are restricted to those parallel to the (100) growth front since *it*-PB1 crystals have facetted morphology indicative of flat growth fronts. At higher ΔT, crystal growth front is kinetically roughened and the chain folding directions are no longer restricted to (100) directions. With increasing temperature, growth front changes from rounded to facetted morphology, which reduces the number of combinations of folding-in and folding-out directions. Reduced number of combinations of folding-in and folding-out directions causes the reduction of configurational entropy of re-entrant sites of folded chains, and this shows up as the higher value of q in the low ΔT range. We can therefore postulate that the change in directional entropy of chain folding was detected in the change in the q values accompanying the transition of l_c.

Acknowledgment. This work was partially supported by "Academic Frontier" Project from MEXT, 2004–2008. The author MY expresses his sincere thanks to Professor Kawaguchi (Ritsumeikan University) and Mr. Masada (Tokuyama Corporation) for GPC measurements, Professor Sawamura (Ritsumeikan University) and Dr. Matsuo (Ritsumeikan University) for their kind instruction in density measurement technique, and Professor Miyaji (Kyoto University) and Professor Fukao (Ritsumeikan University) for valuable discussions and encouragement.

Received: October 31, 2007
Accepted: July 1, 2008
Published: October 15, 2008

REFERENCES

1. J. D. Hoffman, G. T. Davis, and J. I. Lauritzen Jr., in "Treatise on Solid State Chemistry," N. B. Hannay, Ed., Plenum, New York, 1976, Chap. 7, p. 497.
2. J. D. Hoffman and R. L. Miller, *Polymer*, **38**, 3151 (1997).
3. Q. Fu, B. Heck, G. Strobl, and Y. Thomann, *Macromolecules*, **34**, 2502 (2001).
4. M. Yamashita and M. Kato, *J. Appl. Crystallogr.*, **40**, s650 (2007).
5. G. Natta, P. Corradini, and I. W. Bassi, *Nuovo Cimento Suppl.*, **15**, 52 (1960).
6. K. Tashiro, A. Saiani, S. Miyashita, Y. Chatani, and H. Tadokoro, *Polym. Prepr., Jpn.*, **47**, 3869 (1998).
7. R. L. Miller, in "Polymer Handbook," 4th ed., J. Brandrup, E. H. Immergut, and E. A. Grulke, Ed., Interscience Publishers, New York, 1999, Chap. 6, pp VI/7-8.
8. U. Leute and W. Dollhopf, *Colloid Polym. Sci.*, **261**, 299 (1983).
9. M. Yamashita and M. Kato, *J. Appl. Crystallogr.*, **40**, s558 (2007).
10. A. Turner-Jones, *J. Polym. Sci., Part B: Polym. Lett.*, **1**, 455 (1963).
11. M. Yamashita, H. Miyaji, K. Izumi, and A. Hoshino, *Polym. J.*, **36**, 226 (2004).
12. M. Yamashita and T. Takahashi, in "Modern Research and Educational Topics in Microscopy," A. Méndez-Vilas and J. Díaz, Eds., Formatex Research Centre, Badajoz, 2007, p 713.
13. M. Yamashita, A. Hoshino, and M. Kato, *J. Polym. Sci., Polym. Phys. Ed.*, **45**, 684 (2007).
14. M. Yamashita and T. Takahashi, *Kobunshi Ronbunshu*, **65**, 218 (2008).
15. M. Yamashita and S. Ueno, *Cryst. Res. Technol.*, **42**, 1222 (2007).
16. M. Yamashita, *J. Cryst. Growth.*, **310**, 1739 (2008).
17. H. Miyaji, Y. Miyamoto, K. Taguchi, A. Hoshino, M. Yamashita, O. Sawanobori, and A. Toda, *J. Macromol. Sci.*, **B42**, 867 (2003).
18. P. Sonntag, C. M. Care, S. J. Spells, and I. Halliday, *J. Chem. Soc., Faraday Trans.*, **91**, 2593 (1995).
19. M. Kurata and Y. Tsunashima, in "Polymer Handbook" 4th ed., J. Brandrup, E. H. Immergut, and E. A. Grulke, Ed., Interscience Publishers, New York, 1999, Chap. 7, pp VII/48–49.